Journal of Nuclear Materials 393 (2009) 508–512

Contents lists available at ScienceDirect

Journal of Nuclear Materials

journal homepage: www.elsevier.com/locate/jnucmat

First-principles investigation on dissolution and diffusion of oxygen in tungsten

Abdullah Alkhamees, Yue-Lin Liu, Hong-Bo Zhou, Shuo Jin, Ying Zhang, Guang-Hong Lu *

Department of Physics, Beijing University of Aeronautics and Astronautics, Beijing 100191, China

ARTICLE INFO

Article history:
Received 16 April 2009
Accepted 25 July 2009

PACS:
21.10.Dr
21.10.Ft
71.15.Mb
81.05.Bx
61.72.−y

ABSTRACT

Using a first-principles method, we have investigated dissolution and diffusion properties of oxygen (O) in tungsten (W). Single O atom prefers to occupy the tetrahedral interstitial site (TIS). Two interstitial O atoms are attractive and tend to be paired up at two neighboring TIS with a distance of 0.228 nm and a large binding energy of 1.60 eV, which indicates a strong tendency of O clustering in W. O is preferred to diffuse between the most nearest neighboring TIS with a diffusion barrier of 0.17 eV. By the estimation of pre-exponential factor according to an empirical theory, the diffusion coefficient as a function of temperature has been determined, which is 1.50×10^{-9} m^2/s at a typical temperature of 500 K. The results provide a good reference to understand the behavior of O in intrinsic W.

1. Introduction

It is an unquestionable fact that the shortage and the increase of demand of energy in the 21st century have evoked international cooperation to consider other ways to meet the mankind needs. For example, fusion energy, a kind of clean, infinite energy for future generation, has been developed for its construction via ITER Project [1]. Tungsten (W) and W alloys are considered among the most promising plasma facing materials (PFMs) because of their low sputtering erosion and good thermal properties such as high thermal conductivity and high melting temperature. The light elements such as oxygen (O) are regarded as the common impurities in metals. The presence of even very little amount of O impurity, e.g., as low as 30 atomic parts per million (appm) [2–4] in W, can change the microstructure significantly. Further, O can be easily trapped by some extended defects such as vacancies, dislocations and grain boundaries [5], leading to the degradation of the mechanical properties. Moreover, recent experimental studies reported that O can be regarded as the trapping sites, which makes large amount of hydrogen (H) isotope ions aggregate and further form H blisters [6–8]. However, fewer studies have been devoted to understanding the interaction of between O and W, which has a direct impact on the design and operation of the PFM.

The interaction of O with metal as well as metal–alloys is of great scientific and technological interest. In the previous experiments, Hatakeyama et al. studied the diffusion behavior of O in vanadium-alloy [9]. They found that diffusion of O can enhance the precipitations of vanadium-alloy. Filius and van Veen reported the effect of impurity O on the helium (He) retention in W and molybdenum [10]. They found that O can decrease the binding energy between He and vacancy-type cluster. As to theoretical predictions, the electronic structure and bonding properties of O with metal–alloys such as NiAl [11–14] have been investigated using first-principles method since O is considered as one possible reason for the room temperature brittleness of the NiAl. Despite many years of research of O-metal interaction, many fundamental aspects underlying the O-metal interaction are still not fully understood, especially for the behaviors of O in W. Moreover, Understanding O–W interaction will be helpful to understand the effect of O on the structure and diffusion properties of other metals.

In order to understand the physical mechanism underlying the interaction of O with intrinsic W, in this paper, we investigate the structure, energetics, and diffusion properties of O in W using first-principles calculations. This work serves as the first step to investigate the effect of O on the blistering behaviors of H in W.

2. Computational methods

We employ a total-energy method based on density functional theory [15,16] with generalized gradient approximation developed by Perdew and Wang [17] and the projector-augmented-wave potential. We use a kinetic energy cutoff of 350 eV for all calculations. The uniform grids of k-points are sampled by $5 \times 5 \times 5$ for 54-atom supercell and $3 \times 3 \times 3$ for 128-atom supercell. The calculations have been carried out by VASP [18,19]. The calculated equilibrium lattice constant is 0.317 nm for a bcc W, in good agreement with the corresponding experimental value of 0.316 nm. The energy

* Corresponding author. Tel./fax: +86 10 82339917.
E-mail address: lgh@buaa.edu.cn (G.-H. Lu).

0022-3115/$ - see front matter © 2009 Elsevier B.V. All rights reserved.
doi:10.1016/j.jnucmat.2009.07.012

relaxation iterates until the forces on all the atoms are less than 10^{-2} eV/nm.

The solution energy of O point defects in intrinsic W is defined as

$$E^{S}_{defect} = E_{NW,O} - NE_W - \mu(O), \quad (1)$$

where the $E_{NW,O}$ is the total-energy of the supercell containing N W atoms and one O atom, E_W is the energy of an ideal bulk W atom and $\mu(O)$ is the O chemical potential.

The binding energy E_b two O atoms in intrinsic W is defined as

$$E_b = nE_{1O} - E_{2O} - E_{ref}, \quad (2)$$

where E_{1O} and E_{2O} are the energy of the supercell with one tetrahedral interstitial site (TIS) O atom only and two O atoms, respectively, while E_{ref} is the energy of the supercell without O atoms. Here, negative binding energy indicates repulsion among O atoms, while positive indicates attraction.

3. Results and discussion

3.1. Single O atom in intrinsic W

3.1.1. Solution energy of single O atom

The possible sites that O may occupy in intrinsic W include the interstitial and substitutional sites. All the substitutional sites (SS) are equivalent in bcc metals, but the tetrahedral interstitial site (TIS) and the octahedral interstitial site (OIS) differ obviously. For a comparison, we hypothesize the high-symmetry case for the O substitution, i.e., O atom is at the center of SS. The case for O deviation from the substitutional center is related to the O-vacancy interaction, for which the calculations are in process. We have calculated the solution energy of O at the different sites in intrinsic W, as shown in Fig. 1. For O interstitial sites, we consider the high-symmetry cases for both TIS and OIS, i.e., O atom stays at the center of interstitial sites. The O atom is found to be energetically favorable sitting at the TIS with a solution energy of −1.75 eV in reference to the O chemical potential $\mu_O = -2.60$ eV [20]. For O in OIS, the solution energy is −1.43 eV, higher than that of TIS. However, if O atom is slightly off the center of TIS or OIS, O will still go back to the center of TIS; while for OIS case, it always goes towards the TIS after the structure optimization. This suggests that the OIS is not the local energy minimum site for O. This can be further confirmed by the diffusion of O in Section 3.3.

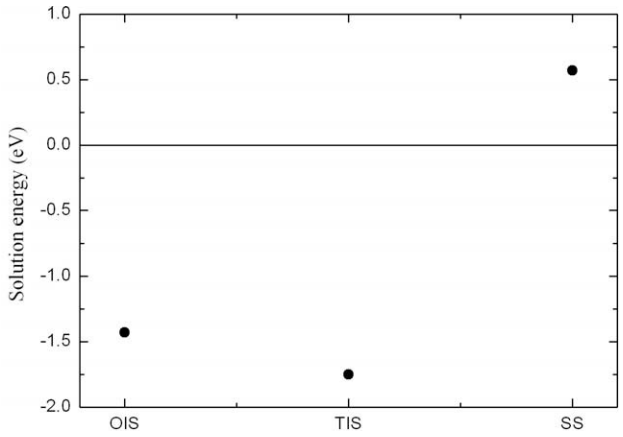

Fig. 1. Solution energies for O atom in OIS, TIS, and SS in bcc W, respectively. The reference energy is taken as the chemical potential of O of −2.60 eV.

3.1.2. Atomic structure and charge density distribution

Valence charge density distribution reflects the bonding characteristics between atoms [21]. Fig. 2 illustrates the charge density distribution map of different structures for the single O in W. W is a transition metal element with four 5d electrons and two 6s electrons. O is a Group VI element with two 2s electrons and four 2p electrons. For all the three cases, the charge density plots show that most of O charge is spatially localized around O. The charge density between the substitution O and W is shown to be very low (Fig. 2a), implying their weak interaction and thus the SS of O in W is unfavorable. This corresponds to the higher solution energy of substitutional O in W as shown above. For both the OIS and TIS cases (Fig. 2b and c), the charge density between O and the first-nearest-neighbor (1NN) W is relatively higher with shorter lengths, suggesting the relatively stronger W–O interaction in comparison with the SS case. However, the charge density is very low between the 2NN W and O due to the larger W–O lengths.

3.1.3. Density of states

Fig. 3 shows the total density of states (DOS) of W with O at the SS, OIS, and TIS, respectively. As compared with the pure W, the total DOS exhibits an additional small peak in the lower-energy part when O is introduced by replacing the W or directly occupying TIS or OIS in W. Moreover, there exists another small peak in the higher energy part for both TIS and OIS. Thus, we can conclude that these small peaks should be directly related to the presence of O. The main peaks close to the Fermi energy should correspond to the W–W bonding according to the DOS of the pure W.

In order to further investigate the origin of these additional peaks that appear in the total DOS due to the presence of O, we have calculated the local density of states (LDOS) of O for 2s and 2p orbital for all these cases, as well as that of the pure O atom. As shown in Fig. 4d, O has two strong characteristic peaks, corresponding to the 2s and 2p orbital, respectively. For the pure O gas, it is well known that the 2p electrons mainly contribute to

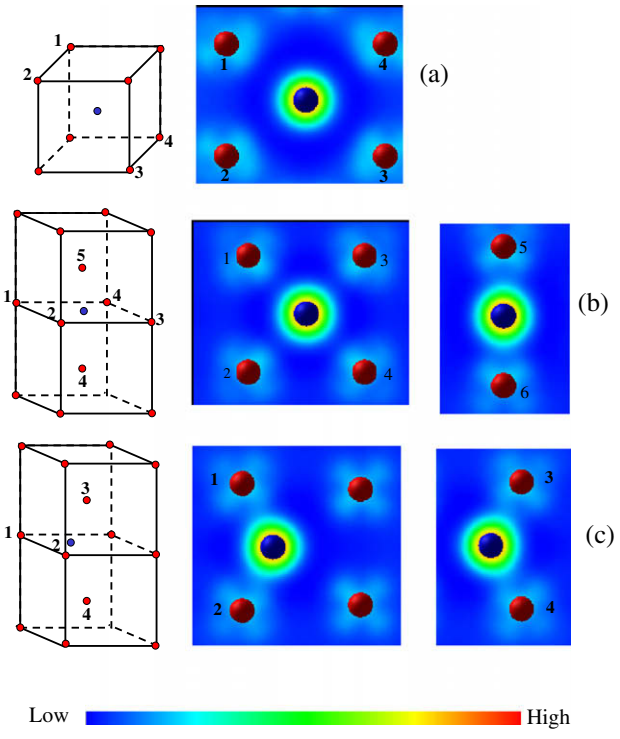

Fig. 2. Atomic structure and valence charge density distribution maps for the cases of (a) substitution site, (b) the OIS, and (c) the TIS, respectively. The larger red balls represent the W atoms and the smaller grey balls represent O atoms.

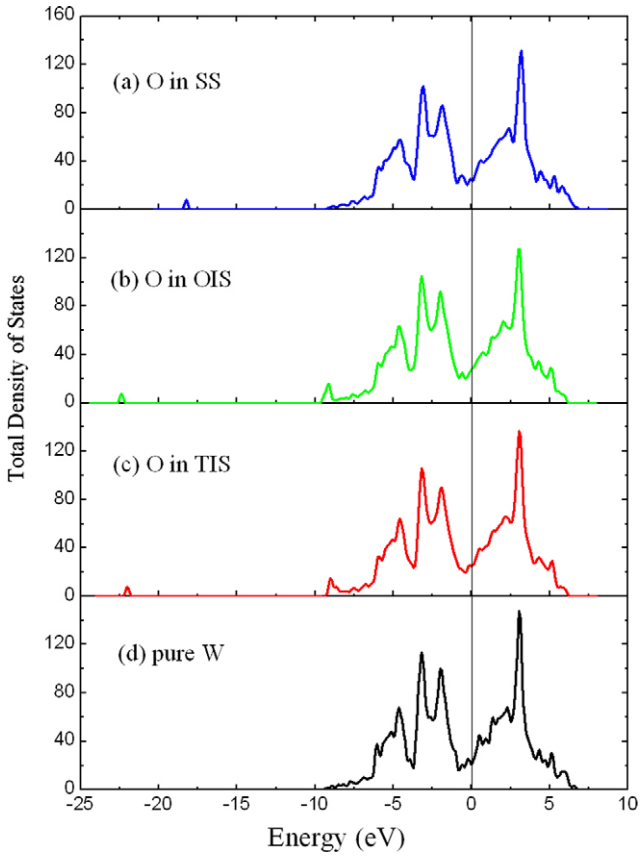

Fig. 3. The total DOS of W with O at the SS, OIS, and TIS, in comparison with that of pure W. The Fermi energy is set to be zero for all the cases.

the O–O bonding, leading to the appearance of a much stronger peak in the higher energy part in the LDOS. However, when O is at substitutional or interstitial sites in W, such stronger peaks in the higher energy part characterizing the 2p electrons of O becomes much weaker and dispersive in the LDOS of O (the blue solid lines in Fig. 4a, b and c), especially for the SS. This is because of the hybridization of O-2p and W-5d that are energetically close to each other as compared with O-2s. The peaks in the lower-energy part (the red solid lines in Fig. 4a, b and c) are similar to that in the LDOS for the pure O atom (the red solid line in Fig. 4d), which is related to the O-2s, although the corresponding energies of these peaks are reduced more or less. Further, the LDOS of O-2p for O in SS notably differs from those of O in OIS and TIS, although in all the three cases O-2p and W-5d present. This suggests the weaker O–W interaction in the SS, corresponding to the lower charge density between O and 1NN W in Fig. 2a. The LDOS results further demonstrate the stronger W–O interaction in both OIS and TIS in W in comparison with the SS case.

Fig. 5 shows the LDOS of W with the presence of O, as well as that of the pure W. W has 5d and 6s valence electrons, which mainly contribute to the interaction of the O–W, especially for the 5d orbitals. When O occupies the SS, the LDOS of the W atoms that is the 1NN O (Fig. 5a) exhibits no obvious variation in comparison with that of the pure W (Fig. 5d). However, the LDOS of the W atom with O in both OIS and TIS are quite different from that in the pure W. Two additional peaks appear in the lower and higher energy parts both for the OIS and TIS cases (Fig. 5b and c). This suggests a stronger W–O interaction as shown in Fig. 2b and c. Moreover, it can be seen that the presence of the additional smaller peak at the lower-energy part for OIS and TIS stem from the interaction of O-2s electrons. Such O-2s electrons do not appear in the SS case. The O–W bonds are thus mainly composed of the O-2p and W-5d electrons.

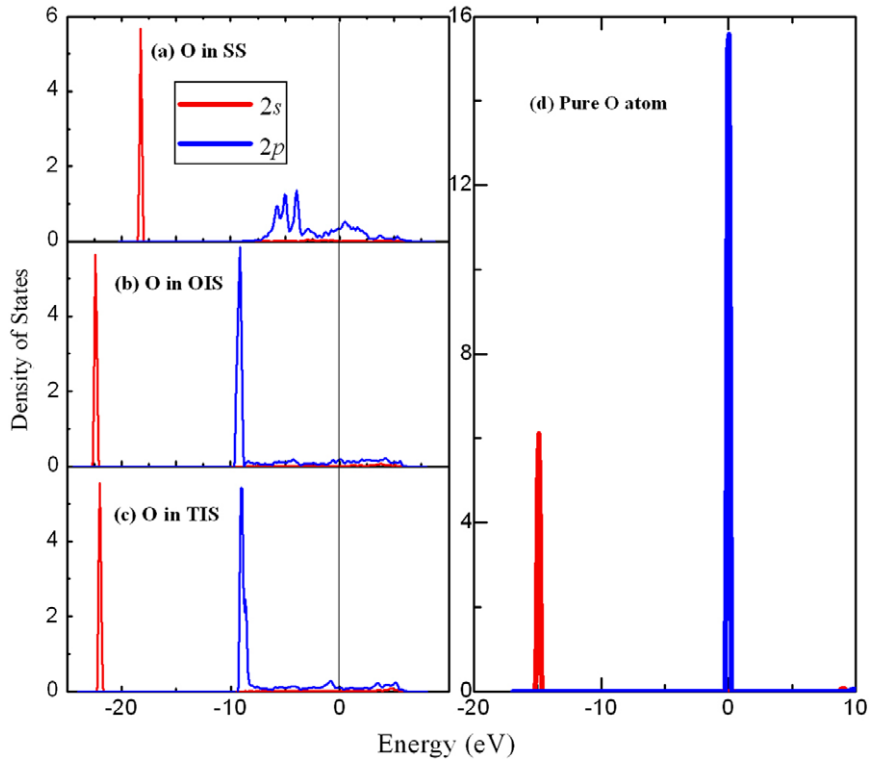

Fig. 4. The LDOS of the O atom in W for different cases in comparison with the pure O atom. (a) SS. (b) OIS. (c) TIS. (d) Pure O atom. The Fermi energy is set to be zero for all the cases.

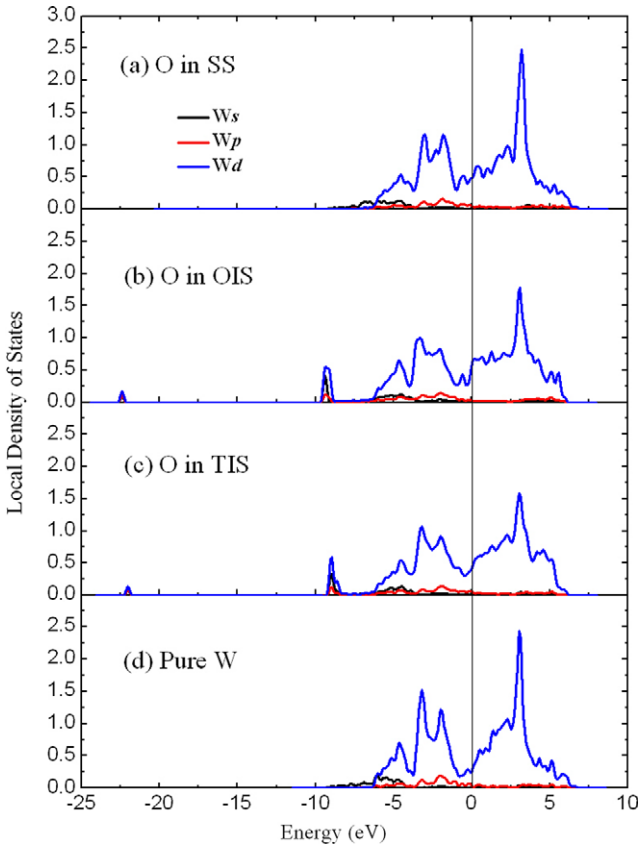

Fig. 5. The LDOS of W regarded as 1NN of the O atom after the O at the SS, OIS and TIS. Fermi energy is set to be zero for all the cases.

3.2. Pairing of O atoms in W

We now turn our attention to the interaction of double O atoms in the intrinsic W. As obtained above, the TIS is most stable for single O atom. We consider different TIS's for two O atoms with different atomic distance in order to investigate such O–O interaction.

A series of calculations shows that two O atoms tend to be paired up at the two neighboring TIS along the ⟨3 1 0⟩ directions with a large binding energy of 1.60 eV, as shown in Fig. 6. The equilibrium distance of such O–O pair is ~0.228 nm. Despite larger binding energy for the O–O pair, the distance of the O–O pair is much longer than the O_2 molecule bond length of ~0.121 nm according to the present calculation. It implies that O atoms cannot directly bind together to form an O_2 molecule in the intrinsic W, but form an O–O pair with the binding energy instead. The possible reason may be that the intrinsic W cannot afford enough free space

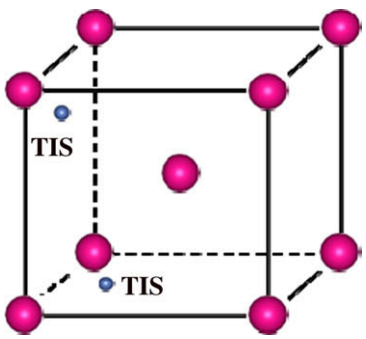

Fig. 6. The most stable configuration for two O atoms.

for the O atom. Further, the pairing of O atoms is shown to be not able to change the atomic configuration of W. Instead, the two O atoms deviate from their respective TIS center. Also, it is clear that two O atoms can easily attract with each other due to the larger binding energy (~1.60 eV), which might lead to the formation of O clusters at higher concentration O impurities in W.

The behavior of O atoms is similar to that of He atoms in the intrinsic W, where they tend to attract directly to each other forming He clusters with the large binding energy of 1.03 eV for two He atoms [22]. Such clustering mechanism will seriously influence the mechanical properties of W. Such clusters might kick out one W atom at high temperature to form one vacancy and self-interstitial atom, i.e., Frenkel-defect pair, even though without vacancy [23].

3.3. Diffusion of O in W

The diffusion properties are quite important for us to understand the clustering behavior of O in W. The diffusion coefficient is an important index to determine the diffusion velocity of O, which helps us to understand the diffusion properties quantitatively. We thus calculate the diffusion energy barrier and determine the diffusion coefficient of O in W.

First, we calculate the energy barrier for single O in TIS which jumps to another TIS in the intrinsic W using a drag method similar

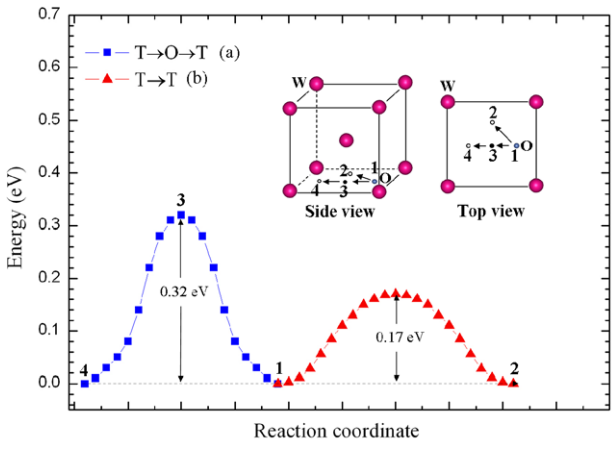

Fig. 7. Diffusion energy profile for interstitial O atom in intrinsic W. (a) T → O → T path. (b) T → T path.

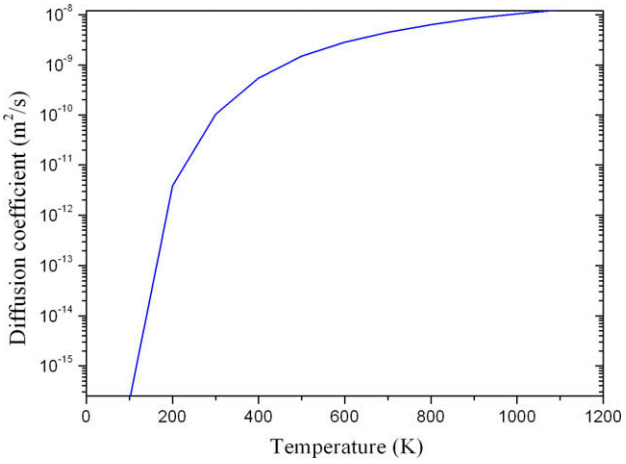

Fig. 8. Diffusion coefficient of O atom via interstitial mechanism as a function of temperature.

Table 1
Diffusion coefficient of O at the temperature from 300 to 1000 K.

T (K)	300	400	500	600	700	800	900	1000
D (m^2/s)	1.05×10^{-10}	5.45×10^{-10}	1.50×10^{-9}	2.82×10^{-9}	4.52×10^{-9}	6.42×10^{-9}	8.45×10^{-9}	1.05×10^{-8}

to the previous studies [24,25]. A possible diffusion path for O is via an OIS between two TIS (T → O → T path). The energy barrier for this path is calculated to be 0.32 eV, as shown in Fig. 7a. The preferred diffusion path for O is via one TIS to another nearest TIS directly (T → T path), as shown in Fig. 7b, with the much lower-energy barrier of 0.17 eV.

Next, we estimate the O diffusion coefficient in W. It is well known that the impurity diffusion coefficient can be obtained by the Arrhenius diffusion equation $D = D_0 \exp(-E_a/kT)$, where the D_0, E_a, k, and T are the pre-exponential factor, activation energy (diffusion energy barrier), the Boltzmann constant, and the absolute temperature, respectively. For a metal with a cubic structure, D_0 can be expressed as $D_0 = \frac{1}{6}a^2\nu$, where a and ν are the lattice constant and the vibration frequency, respectively.

The vibration frequency ν of the interstitial O atom can be determined in two ways. First, according to the harmonic transition state theory [26], $\nu = \prod_{i=1}^{3N}\nu_i / \prod_{i=1}^{3N-1}\nu_i^+$, where ν_i and ν_i^+ are the vibration modes in the initial site (TIS for the present case) and transition state site for O atom, respectively. By constructing and diagonalizing a small Hessian matrix which includes only O and the nearest W atoms, we can obtain the values of ν_i and ν_i^+, and thus ν can be determined. Secondly, we can calculate the vibration frequency ν according to Zener and Wert's theory [27]. In the theory, ν can be approximately expressed by $\nu = \sqrt{2E_a/ma^2}$, where m is the mass of impurity atom.

Here we employ the Zener and Wert's theory to calculate the vibration frequency. Using the mass of O atom of 2.66×10^{-26} kg and the W lattice constant of 3.17×10^{-10} m as well as the calculated O diffusion energy barrier of 0.17 eV, we can thus obtain the vibration frequency $\nu = 4.51 \times 10^{12}$/s. Substituting this value into the diffusion equation, the pre-exponential factor D_0 is obtained, which is 7.57×10^{-8} m^2/s.

With the determination of the pre-exponential factor, the O diffusion coefficient can be calculated according to the Arrhenius equation as explained above. Fig. 8 shows the diffusion coefficient of O as a function of temperature. Apparently, the diffusion coefficient increases with the temperature increasing. The representative coefficients at the temperature from 300 to 1000 K are listed in Table 1. D is shown to be 1.50×10^{-9} m^2/s at a typical temperature of 500 K.

Because few experimental or the relevant calculation data can be found, here we provide a quite useful reference to quantitatively understand the diffusion properties of O in intrinsic W.

4. Summary

We have investigated dissolution and diffusion properties of O in tungsten (W) using a first-principles method based on the density functional theory. Single O atom is energetically favored to occupy the tetrahedral interstitial site (TIS). Two interstitial O atoms are attractive and tend to be paired up at two neighboring TIS along the ⟨3 1 0⟩ direction with a distance of 0.228 nm and a large binding energy of 1.60 eV, which indicates a strong tendency of O clustering in W. O is preferred to diffuse between the most nearest neighboring TIS with a diffusion barrier of 0.17 eV. We employ the Zener and Wert's theory to estimate the pre-exponential factor, and determine the diffusion coefficient as a function of temperature according to the Arrhenius diffusion equation. The diffusion coefficient of O in W is 1.50×10^{-9} m^2/s at a typical temperature of 500 K. The results provide a good reference to understand the behavior of O in the intrinsic W.

Acknowledgements

This work is supported by the National Natural Science Foundation of China (NSFC) with Grant No. 50871009 and ITER Special Project with Grant No. 2009GB106003. Yue-Lin Liu thanks for the support of the Innovation Foundation of BUAA for PhD Graduates.

References

[1] The Fusion Energy is Being Developed Internationally via the ITER (International Thermonuclear Experimental Reactor) Project.
[2] M. Poon, A.A. Haasz, J.W. Davis, J. Nucl. Mater. 374 (2008) 390.
[3] G.-N. Luo, W.M. Shu, M. Nishi, J. Nucl. Mater. 347 (2005) 111.
[4] W.M. Shu, E. Wakai, T. Yamanishi, Nucl. Fusion 47 (2007) 201.
[5] W.T. Geng, Yu-Jun Zhao, A.J. Freeman, B. Delley, Phys. Rev. B 63 (1992) 060101.
[6] M.Y. Ye, H. Kanehara, S. Fukuta, N. Ohno, S. Takamura, J. Nucl. Mater. 313–316 (2003) 72.
[7] K.O.E. Henriksson, K. Nordlund, A. Krasheninnikov, J. Keinonen, Appl. Phys. Lett. 87 (2005) 163113.
[8] Y.-L. Liu, Y. Zhang, H.-B. Zhou, G.-H. Lu, F. Liu, G.-N. Luo, Phys. Rev. B 79 (2009) 172103.
[9] M. Hatakeyama, S. Tamura, T. Muroga, N. Yoshida, M. Hasegawa, H. Matsui, J. Nucl. Mater. 367–370 (2007) 882.
[10] H.A. Filius, A. van Veen, J. Nucl. Mater. 144 (1987) 1.
[11] X.-L. Hu, Y. Zhang, G.-H. Lu, T.M. Wang, J. Phys.: Condens. Matter 21 (2009) 025402.
[12] X.-L. Hu, Y. Zhang, G.-H. Lu, T.M. Wang, P.-H. Xiao, P.-G. Yin, H.B. Xu, Intermetallics 17 (2009) 358.
[13] L.-H. Liu, Y. Zhang, X.-L. Hu, G.-H. Lu, J. Phys.: Condens. Matter 21 (2009) 015002.
[14] X.-L. Hu, Y. Zhang, G.-H. Lu, T.M. Wang, Scr. Mater. 61 (2009) 189.
[15] G.P. Hohenberg, W. Kohn, Phys. Rev. 136 (1964) B864.
[16] W. Kohn, L.J. Sham, Phys. Rev. 140 (1965) A1133.
[17] J.P. Perdew, Y. Wang, Phys. Rev. B 45 (1992) 13244.
[18] G. Kresse, J. Hafner, Phys. Rev. B 47 (1993) 558.
[19] G. Kresse, J. Furthmüller, Phys. Rev. B 54 (1996) 11169.
[20] C. Kittel, Introduction to Solid State Physics, seventh ed., Wiley, New York, 1996.
[21] G.-H. Lu, S.H. Deng, T.M. Wang, Phys. Rev. B 69 (2004) 134106.
[22] C.S. Becquart, C. Domain, Phys. Rev. Lett. 97 (2006) 196402.
[23] F. Gao, H.L. Heinisch, R.J. Kurtz, J. Nucl. Mater. 367–370 (2007) 446.
[24] Y.-L. Liu, Y. Zhang, G.-N. Luo, G.-H. Lu, J. Nucl. Mater. 390–391 (2009) 1032.
[25] C.C. Fu, F. Willaime, P. Ordejon, Phys. Rev. Lett. 92 (2004) 175503.
[26] G.H. Vineyard, J. Phys. Chem. Solids 3 (1957) 121.
[27] R. Frauenfelder, J. Vac. Sci. Technol. 6 (1969) 388.